The electron density and spin magnetic moment of relativistic collinear ferromagnets



1996 J. Phys.: Condens. Matter 8 591

(http://iopscience.iop.org/0953-8984/8/5/009)

J. Phys.: Condens. Matter **8** (1996) 591–602. Printed in the UK

# The electron density and spin magnetic moment of relativistic collinear ferromagnets

N A Shilkova and V P Shirokovskii

Physico-Technical Institute, Russian Academy of Sciences, Ural Branch, 132, Kirov Street, SU-426001, Izhevsk, Russia†

Received 17 July 1995

**Abstract.** An effective technique for computation of the electron density and spin magnetic moment in a ferromagnet, based on the relativistic Korringa–Kohn–Rostoker method, is developed and realized. The calculation formulae are derived using the Hellmann–Feynman theorem and perturbation theory for matrices. The influence of spin–orbit interaction on the formation of the electron spectrum as well as the problem of compatibility of electron states are discussed. The electron density and spin moment distributions and s-, p-, d-type contributions to them are analysed.

## 1. Introduction

A theoretical scheme for calculating the electron spectra of magnetics based on the Dirac equation has been described in basic papers [1, 2]. Many results have already been obtained by following the suggested approach which gained wide acceptance.

More recently we proposed [3] a somewhat different technique for calculating the electron states of a collinear ferromagnet based on a relativistic version of the Green function method [4, 5]. Unlike Feder, Strange and co-workers [1, 2], who considered the band theory problem as a scattering one, we made use of the conventional representation of the electron states in a crystal in terms of the energy eigenvalue spectrum and the wave eigenfunctions.

The treatment of the problem is based on the Dirac equation

$$\left(\hat{H}_0 + \Delta V \hat{\Sigma}\right) \Psi = \varepsilon \Psi. \tag{1}$$

Here $\hat{H}_0$ is the Dirac operator

$$\hat{H}_0 = c\hat{\boldsymbol{\alpha}}\boldsymbol{p} + mc^2\hat{\beta} + V\hat{I}. \tag{2}$$

The term $\Delta V\,\hat{\boldsymbol{\Sigma}}$ ensures the spin polarization;

$$\hat{\boldsymbol{\alpha}} = \begin{pmatrix} 0 & \hat{\boldsymbol{\sigma}} \\ \hat{\boldsymbol{\sigma}} & 0 \end{pmatrix} \qquad \hat{\beta} = \begin{pmatrix} \hat{I} & 0 \\ 0 & -\hat{I} \end{pmatrix} \qquad \hat{\boldsymbol{\Sigma}} = \begin{pmatrix} \sigma_z & 0 \\ 0 & \sigma_z \end{pmatrix} \tag{3}$$

where $\sigma_x$, $\sigma_y$, $\sigma_z$ are the Pauli matrices, and $\hat{I}$ is the unit matrix; and the atomic system of units with energy in Ryd is used, so that $m = \frac{1}{2}$, $c = 274.072\ldots$.

† E-mail address: arg@otf.fti.udmurtia.su.

0953-8984/96/050591+12$19.50  

In the *muffin-tin* (MT) approximation for the potentials $V$ and $\Delta V$ a convenient representation of the four-component spinor $\Psi$ can be obtained only inside the MT sphere:

$$\Psi = \sum_{\substack{l,\mu \\ \nu=1,2}} \mathrm{i}^l C_{l\mu,\nu} \begin{pmatrix} \psi_{l\mu,\nu} \\ -\mathrm{i}\tilde{\psi}_{l\mu,\nu} \end{pmatrix} \tag{4}$$

where

$$\psi_{l\mu,\nu} = \begin{pmatrix} g_{l\mu,\nu+} Y_{lm} \\ g_{l\mu,\nu-} Y_{lm'} \end{pmatrix} \tag{5a}$$

$$c\tilde{\psi}_{l\mu,\nu} = \left(1 + \frac{E - V}{c^2}\right)^{-1} (\hat{\boldsymbol{\sigma}}\boldsymbol{\nabla})\psi_{l\mu,\nu}. \tag{5b}$$

$C_{l\mu,\nu}$ are undetermined coefficients, $g_{l\mu,\nu\pm}$ are solutions of a set of radial equations (see [3], equation (13)), $Y_{lm}$ are spherical harmonics, $m = \mu - 1/2$, $m' = \mu + 1/2$, the signs $\pm$ labelling $g$ denote the spin direction, and $E = \varepsilon - mc^2$.

It should also be noted that relation (5*b*) is approximate, since the term $\Delta V/c^2$ is dropped in the first brackets on the right-hand side. Therein lies our main approximation.

In the outer part of a crystalline cell the representation of $\Psi$ is too unwieldy to be used in calculating the matrix elements of any operators by direct integration over the cell. At the same time some physical characteristics may be obtained without recourse to explicit finding of $\Psi$. In the present publication we propose a way to evaluate the share of the electron density that falls within the MT sphere, the spin component of the magnetization and its MT part without calculating $\Psi$.

Further, the technique developed is used for calculating the density and magnetization in ferromagnetic iron (FM-Fe). Iron, as an ideal collinear ferromagnet, has become in a sense a model material for the study of the influence of relativistic effects on the formation of magnetic properties in metals. Within the last few years many papers have been devoted, in particular, to investigations of characteristic features of the (FM-Fe) electron structure, based on a consistent relativistic *ab initio* calculation. It is not our intention to review all these papers; we shall refer only to those [6–9] whose results can be correlated with ours. The structure of the paper is as follows. The principal mathematical statements are given in section 2. In section 3 we discuss the influence of spin–orbit interaction on the formation of the FM-Fe spectrum, and especially the problem of state compatibility which, in our opinion, has not received sufficient attention in previous publications. The distribution of the electron density and spin moment inside the MT sphere—depending on the state—is considered in section 4, as well as the contributions of s, p and d type in total magnitudes. Section 5 is devoted to some peculiarities of the formation of the total spin magnetic moment. A brief general summary is given in section 6.

The results presented in this publication have been obtained using the same model and approximations as in our earlier paper [10]. All tabulated values are accurate to $(1\text{–}2)\times 10^{-4}$.

## 2. Statement of the general principle

Let the potential $V$ in equation (1) be assigned a small constant increment $\Delta$, which differs from zero inside the MT sphere. Then in the first order of perturbation theory

$$\Delta\varepsilon \int_{\Omega_{WS}} \Psi^\dagger \Psi \, \mathrm{d}\boldsymbol{r} = \Delta \int_{\Omega_{MT}} \Psi^\dagger \Psi \, \mathrm{d}\boldsymbol{r} \tag{6}$$

where $\Omega_{WS}$ and $\Omega_{MT}$ are the volumes of the Wigner–Seitz (WS) cell and the MT sphere, respectively. As $\Delta$ tends to zero, we obviously have

$$\omega = \frac{\partial \varepsilon}{\partial \Delta} = \int_{\Omega_{MT}} \Psi^{\dagger}\Psi \, \mathrm{d}\boldsymbol{r} \Big/ \int_{\Omega_{WS}} \Psi^{\dagger}\Psi \, \mathrm{d}\boldsymbol{r} \tag{7}$$

i.e. $\omega$ represents the share of the density within the MT sphere. Thus, having specified the procedure for finding the derivative in equation (7), we obtain a $\Psi$-independent technique for calculating the MT share of the electron density, i.e. its degree of localization, depending on the type of the state.

If now the small constant increment $\Delta$ is assigned to the potential $\Delta V$ in (1), we have

$$\Delta\varepsilon \int_{\Omega_{WS}} \Psi^{\dagger}\Psi \, \mathrm{d}\boldsymbol{r} = \Delta \int_{\Omega_{WS}} \Psi^{\dagger}\hat{\boldsymbol{\Sigma}} \, \Psi \, \mathrm{d}\boldsymbol{r}. \tag{8}$$

Further, depending on whether the increment $\Delta$ is nonzero everywhere over the WS cell or only inside the MT sphere, we get two limiting relations:

$$S_z = \frac{\partial \varepsilon}{\partial \Delta} = \int_{\Omega_{WS}} \Psi^{\dagger}\hat{\boldsymbol{\Sigma}}\Psi \, \mathrm{d}\boldsymbol{r} \Big/ \int_{\Omega_{WS}} \Psi^{\dagger}\Psi \, \mathrm{d}\boldsymbol{r} \tag{9}$$

and

$$S_{MT} = \frac{\partial \varepsilon}{\partial \Delta} = \int_{\Omega_{MT}} \Psi^{\dagger}\hat{\boldsymbol{\Sigma}}\Psi \, \mathrm{d}\boldsymbol{r} \Big/ \int_{\Omega_{WS}} \Psi^{\dagger}\Psi \, \mathrm{d}\boldsymbol{r}. \tag{10}$$

The first equation gives the total mean value of the spin moment projection onto the O$z$ axis for a given state, while the second defines its MT share. And again the problem reduces to the calculation of some energy derivatives with respect to the parameter. We have repeatedly used this simple expedient when normalizing the wavefunctions [11], and calculating the velocities [12] and the effective mass [13].

The main dispersive equation for a relativistic ferromagnet has the form (see [3], equation (22))

$$\begin{vmatrix} A + W^{+} & W \\ W^{\dagger} & A + W^{-} \end{vmatrix} = 0 \tag{11}$$

where the $A$ are the potential-independent matrices of structure constants, whose explicit analytical form is contained in [14]; $W^{\pm}$, $W$ are relativistic cotangents of scattering phases, for which explicit expressions are given in [3], equations (23)–(25).

It is known that for dispersive equations like (11) the energy eigenvalues $\varepsilon_n(\boldsymbol{k})$ are found subject to the condition that an eigenvalue $\lambda_j(E)$ of the corresponding matrix is equal to zero. In the problem under consideration this $\lambda_j$ will depend on the parameter $\Delta$ both explicitly and through the dependence of the energy on this parameter. At the same time the condition

$$\lambda_j\big(\varepsilon_n(\boldsymbol{k}, \Delta), \Delta\big) = 0 \tag{12}$$

should be fulfilled at any value of $\Delta$. Then, obviously

$$\frac{\partial \varepsilon_n}{\partial \Delta} = -\frac{\partial \lambda_j}{\partial \Delta} \Big/ \left(\frac{\partial \lambda_j}{\partial E}\right)_{E=\varepsilon_n}. \tag{13}$$

Thus, mathematically the problem reduces to calculating the derivatives of the eigenvalue $\lambda_j$ of matrix (11) with respect to the parameter $\Delta$ and the energy $E$.

Denote the matrix elements of (11) by $H_{lms,l'm's'}$ and let $t_j$ be the eigenvector of this matrix corresponding to the eigenvalue $\lambda_j$. Then

$$\frac{\partial \lambda_j}{\partial \Delta} = \sum_{\substack{lms \\ l'm's'}} t^*_{j,lms} \frac{\partial H_{lms,l'm's'}}{\partial \Delta} t_{j,l'm's'}. \tag{14}$$

For $\partial\lambda_j/\partial E$ the procedure is quite analogous. Let us note that simultaneously with calculation of $\omega$ and $S_{MT}$ one can compute also the partial—i.e. corresponding to fixed $l$—shares $\omega_l$ and $S_l$. To this end it is sufficient to carry out in (14) summation over $m, s$ and $m', s'$ with $l$ fixed.

In what follows, we shall not pay attention to mathematical aspects. The detailed mathematical manipulations, though elementary, are rather cumbersome routines and contribute but little to the main point of the paper.

## 3. Peculiarities of the ferromagnetic iron spectrum formation within the relativistic scheme

In what follows the unit cell of FM-Fe will be considered as a Wigner–Seitz (WS) cell. The Brillouin zone (BZ) is assumed to have a standard bcc form with points and directions of $\boldsymbol{k}$-space given in Bouckaert, Smoluchowskii and Wigner notation [15]. We also assume that the magnetization vector lies in the O$z$ axis. Thus, it is significant that in the subsequent discussion the O$z$ axis is the tetrad one.

If the O$z$ axis were an axis of 'infinite-order' symmetry, the projection of the total angular momentum onto it, $J_z$, would be a conserved quantity (quantum number), $\mu$. Since in FM-Fe it is only the rotation through a finite angle $\pi/2$ (and its multiples), denoted as $\hat{J}_z(\pi/2)$, that commutes with the Dirac operator $\hat{H}_D$ (see (1)), the eigenfunctions $\Psi$ can be chosen so that

$$\hat{J}_z(\pi/2)\Psi = \mathrm{e}^{\mathrm{i}\mu\pi/2}\Psi. \tag{15}$$

In other words, the conserved quantities that take the place of $\mu$ will be $\mathrm{e}^{\mathrm{i}\mu\pi/2}$. Since, however,

$$\mathrm{e}^{\mathrm{i}\mu\pi/2} = \mathrm{e}^{\mathrm{i}\mu'\pi/2} \tag{16}$$

if

$$\mu - \mu' \equiv 0 \qquad (\mathrm{mod}\, 4) \tag{17}$$

the angular momentum projection $\mu$ is defined in accordance with the comparison equation (17), i.e. we can put $\tilde{\mu} = \pm 1/2, \pm 3/2$ and classify all the states of $\Psi$ with respect to the value of $\tilde{\mu}$.

At the BZ points of general type, there is little sense in classifying the states on the basis of point symmetry operations. If, however, such operators are involved in the group of wavevector $\boldsymbol{k}$, some additional information about the state behaviour may be obtained. (It is not our intention to perform a full group analysis of the problem, the above consideration being quite sufficient for what follows. Closer examination of the problem can be found in [16].) Consider, for example, the states with a wavevector $\boldsymbol{k}$, directed along the O$z$ axis. In this case the wavevector group involves a tetrad axis and all four types of state are realized according to the value of $\tilde{\mu}$. To denote these states we shall use the symbol $\Delta^{\parallel}(\tilde{\mu})$. Passing to the points of higher symmetry $\Gamma$ and H does not substantially change the situation, because the possible different types of state do not increase in number and again they may be specified by the index $\tilde{\mu}$.

When considering the states with the wavevector directed along the O$y$ (or O$x$) axis, the number of state types reduces to two by virtue of symmetry lowering. Again, for reasons of symmetry we could introduce some $\tilde{\mu}$, defined with an accuracy comparable in mod 2. (More precisely, $\tilde{\mu}$ would equal $\pm\frac{1}{2}(-1)^l$.) It is more convenient to use the indices $\pm$, introducing the notation $\Delta^{\perp}(\pm)$.

Because the states of different types do not interact, the corresponding dispersion curves can intersect—that is, an accidental degeneracy may occur along the $\Delta$ direction. Since the numbers of noninteracting states are different for $\Delta^{\parallel}$ and $\Delta^{\perp}$ directions, the compatibility of states must of necessity differ as well. As an illustration, we shall consider a group of states which are identified as d-type states at the points $\Gamma$ and H of the BZ. The energy values at geometrically identical points of the BZ are listed in table 1 for the $\Delta^{\parallel}$ and $\Delta^{\perp}$ directions. One can see that the numerical values of the terms presented differ by no more than 2–3 mRyd. The same is true for all other points $\boldsymbol{k}$ along this direction—in other words, the energy changes connected with different orientations of $\boldsymbol{k}$ with respect to the magnetization direction are small for Fe, as was to be expected.

**Table 1.** Energy values (in mRyd) at the points $\boldsymbol{k} = (\pi/a)(001)$ (i.e. $\Delta^{\parallel}$) and $\boldsymbol{k} = (\pi/a)(010)$ (i.e. $\Delta^{\perp}$). The magnetic moment lies in the O$z$ direction.

| | | | | Term type[b] | |
|---|---|---|---|---|---|
| $\mu$[a] | $\tilde{\mu}$ | $\Delta^{\parallel}$ | $\Delta^{\perp}$ | (c) | (d) |
| −3/2, 5/2 | −3/2 | 366.3 | 366.3 | + | + |
| −1/2 | −1/2 | 421.9 | 424.1 | − | − |
| 3/2, −5/2 | 3/2 | 426.6 | 424.3 | + | − |
| −3/2, 5/2 | −3/2 | 472.5 | 471.6 | − | + |
| 3/2, 5/2 | 3/2 | 490.9 | 491.8 | − | − |
| 1/2 | 1/2 | 555.7 | 558.7 | + | + |
| −3/2, 5/2 | −3/2 | 562.2 | 559.8 | − | + |
| 1/2 | 1/2 | 574.4 | 573.8 | + | + |
| 3/2, −5/2 | 3/2 | 620.4 | 620.4 | + | − |
| −1/2 | −1/2 | 698.2 | 698.2 | − | − |

[a] Values of $\mu$ involved ln the wave-function expansion for the given energy in the case $\Delta^{\parallel}$ ($l \leqslant 2$).

[b] In the wave-function expansion the following values of $\mu$ correspond to the sign '+': $l = 0, \mu = 1/2$; $l = 1, \mu = -1/2, 3/2$; $l = 2, \mu = -3/2, 1/2, 5/2$; while $l = 0, \mu = -1/2$; $l = 1, \mu = -3/2, 1/2$; $l = 2, \mu = -5/2, -1/2, 3/2$ correspond to '−'.

[c] The type of state which actually corresponds to the given energy.

[d] The type of state which should correspond to the given $\Delta^{\parallel}(\tilde{\mu})$ for reasons of symmetry.

The situation, however, appears to be more complicated when the general run of dispersion curves is considered. The dispersion curves corresponding to two groups of noninteracting states are shown in figure 1. For the $\Delta^{\perp}$ direction the states of each group are interacting and the relevant dispersion curves cannot cross.

For the $\Delta^{\parallel}$ direction the groups considered contain in each case two types of state, which are represented by different lines in figure 1. We see that the graphical picture has undergone substantial changes. Crossing curves of different types appear, as well as curves that almost merge together. Using solid and dashed lines to plot the curves on the right in both parts of figure 1, we wanted to emphasize interrelation of different branches of dispersion curves. It should be noted that all one needs to do in order to obtain a complete spectrum pattern is to superimpose the two halves of figure 1 (given on facing pages). Then,

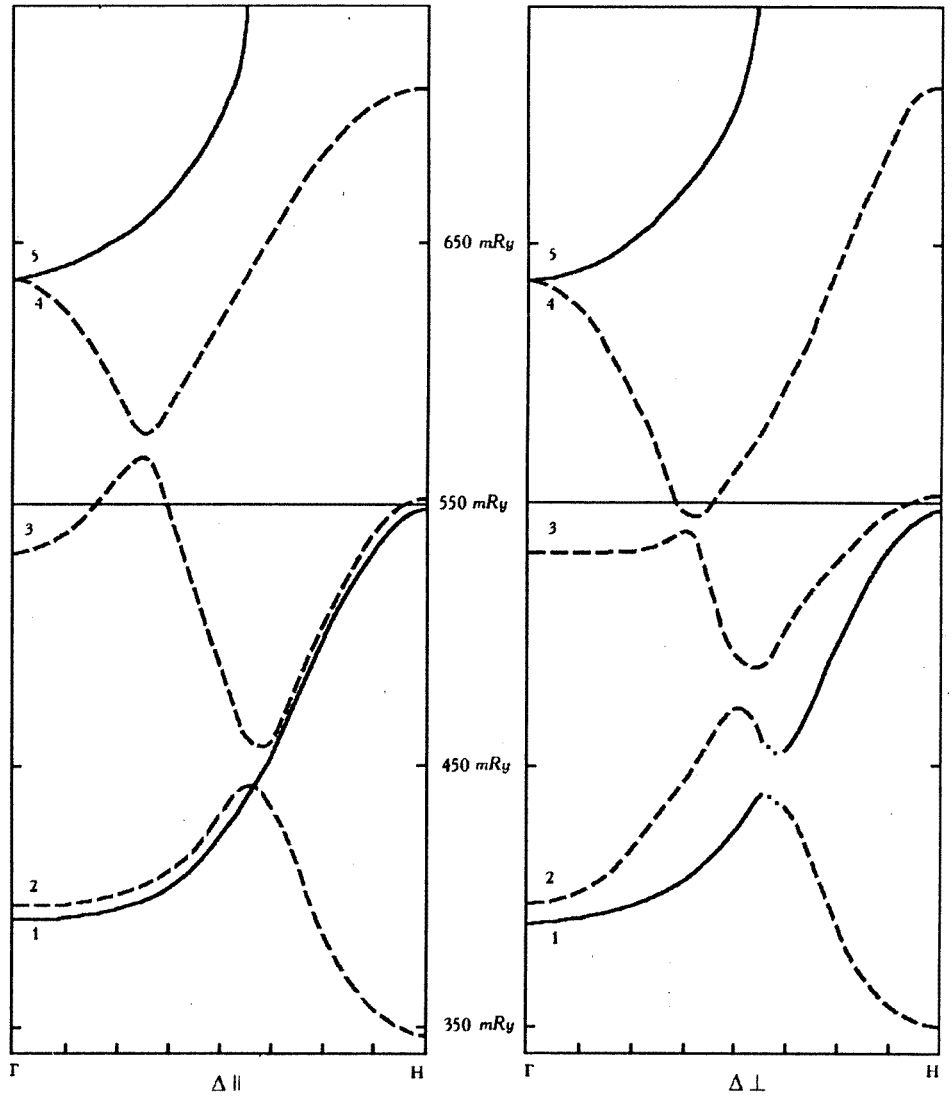


**Figure 1.** This page: dispersion curves along Δ directions: the left-hand side corresponds to $\Delta^{\parallel}(-1/2)$ (solid curves), and $\Delta^{\parallel}(3/2)$ (dashed curves); while the right-hand side corresponds to $\Delta^{\perp}(-)$. Facing page: as on this page, except that the left-hand side corresponds to $\Delta^{\parallel}(1/2)$ (solid curves), $\Delta^{\parallel}(-3/2)$ (dashed curves); while the right-hand side coresponds to $\Delta^{\perp}(+)$.

quite obviously, the meeting and closely spaced curves markedly grow in number.

## 4. The electron density and spin moment inside the MT sphere

The MT share of the electron density for a given state and the corresponding spin magnetic moment were found according to (7) and (10). Let us recollect that, when using the MT approximation for the potential, it is useful to calculate also the contribution of s, p and d states to the total magnitude.

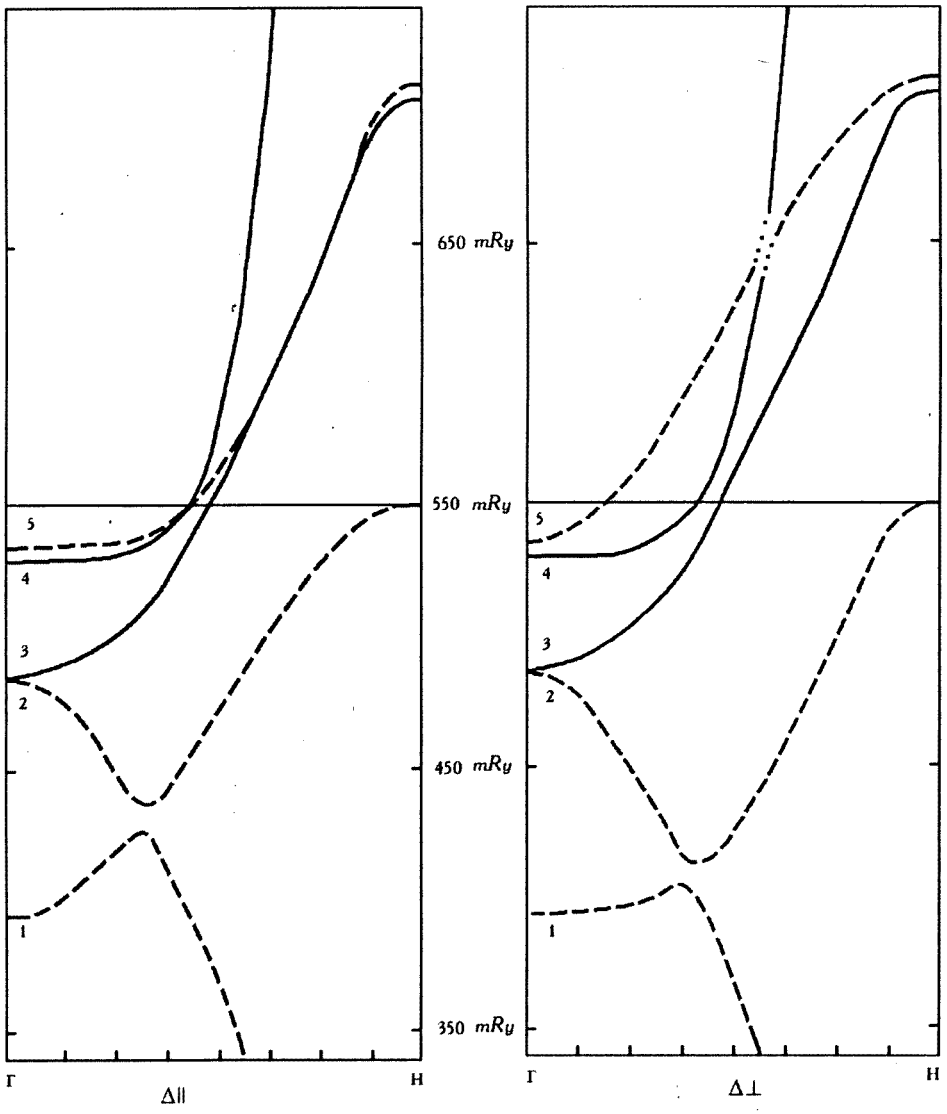


**Figure 1.** (Continued)

The results of calculation at points $\boldsymbol{k} = (\pi/a)(001)$ and $\boldsymbol{k} = (\pi/a)(010)$ of the BZ for a group of bands corresponding mainly to the d states are given in table 2. We begin our consideraion with the states $\Delta^{\|}(\tilde{\mu})$.

Although it is evident from the data presented that the main contribution to the density comes from the d states, individual states exhibit some distinct features. So for the states listed in rows 1–4, 7 and 9 of the table, the MT sphere accounts for more than 90% of the d-electron density. For the states in rows 6, 8 and 10 a reduction in the share of d electrons is mainly due to the appearance of s and p additions. The data in row 5, however, show that even with a negligible hybridization the degree of delocalization (smearing) of the d function may amount to more than 10%.

**Table 2.** Total and partial electron densities inside the MT sphere and corresponding to spin magnetic moment values (in $\mu_B$). All the magnitudes are listed for the same energies as in table 1 (the types of energy term $\Delta^{\parallel}(\tilde{\mu})$ and differences $E^{\parallel} - E^{\perp}$ (in mRyd) are listed in the first column; the following columns contain $\omega_0^{\parallel}$, $\omega_1^{\parallel}$, etc and $\omega_0^{\parallel} - \omega_0^{\perp}$, $\omega_1^{\parallel} - \omega_1^{\perp}$, etc).

| Term | $\omega_0$ | $\omega_1$ | $\omega_2$ | $\omega$ | $S_0$ | $S_1$ | $S_2$ | $S_{MT}$ |
|---|---|---|---|---|---|---|---|---|
| $\Delta^{\parallel}(-3/2)$ | 0[a] | — | 0.912 | 0.912 | 0 | — | 0.912 | 0.912 |
| — | — | — | — | — | — | — | — | — |
| $\Delta^{\parallel}(-1/2)$ | — | 0.023 | 0.934 | 0.957 | — | 0.023 | 0.934 | 0.957 |
| **−2.2**[b] | — | — | — | — | — | — | **0.003** | **0.003** |
| $\Delta^{\parallel}(3/2)$ | 0 | 0.023 | 0.934 | 0.957 | 0 | 0.023 | 0.930 | 0.953 |
| 2.3[c] | — | — | — | — | — | — | **−0.003** | **−0.003** |
| $\Delta^{\parallel}(-3/2)$ | 0 | — | 0.979 | 0.979 | 0 | — | 0.977 | 0.977 |
| **0.9** | — | — | **0.004** | **0.004** | 0 | — | **0.083** | **0.083** |
| $\Delta^{\parallel}(3/2)$ | 0 | — | 0.891 | 0.891 | 0 | — | −0.887 | −0.887 |
| **−0.9** | — | — | **−0.004** | **−0.004** | — | — | **−0 082** | **−0.082** |
| $\Delta^{\parallel}(1/2)$ | 0.013 | 0.034 | 0.896 | 0.943 | 0.013 | −0.021 | −0.766 | −0.774 |
| −3.0 | 0.004 | 0.001 | −0.006 | −0.001 | 0.004 | 0.002 | 0.041 | 0.047 |
| $\Delta^{\parallel}(-3/2)$ | 0 | 0.030 | 0.917 | 0.947 | 0 | −0.030 | −0.914 | −0.944 |
| **2.4** | — | — | — | — | — | — | — | — |
| $\Delta^{\parallel}(1/2)$ | 0.124 | 0.063 | 0.732 | 0.919 | 0.124 | 0.057 | 0.561 | 0.742 |
| 0.6 | −0.003 | −0.001 | 0.006 | 0.002 | −0.003 | −0.003 | −0.041 | −0.047 |
| $\Delta^{\parallel}(3/2)$ | 0 | — | 0.975 | 0.975 | 0 | — | −0.974 | −0.974 |
| — | — | — | — | — | — | — | — | — |
| $\Delta^{\parallel}(-1/2)$ | 0.093 | 0.038 | 0.818 | 0.949 | −0.093 | −0.038 | −0.817 | −0.948 |
| — | — | — | — | — | — | — | — | — |

[a] '0' corresponds to the precise zero value; '—' denotes that the value is beyond the calculational accuracy.

[b,c] The quantities corresponding to different groups of noninteracting states for $\Delta^{\perp}$ are printed in different type-faces.

At the same time we can see that, as a rule, the absolute magnitude of the spin moment follows the density. Small deviations of the spin-momentum values—namely their decreasing—can be readily explained, e.g., by interaction of the spin of an electron with its own 'orbital' motion. The exception is provided by the states in rows 6 and 8. Here a pronounced decrease (in magnitude) of the spin moment is due to strong interaction of $\Delta^{\parallel}(1/2)$ states of the same type with different spin orientations. In other words, both states are mixed in spin, the opposite-in-sign component being present at all $l$, which is evident from comparison of the quantities $\omega_l$ and $S_l$.

The analysis of changes in density and spin moment which arise when passing to $\boldsymbol{k} = (\pi/a)(010)$ lends further support to our conclusions. First of all we should mention that when the terms of the same type are separated by more than 50 mRyd (rows 1, 7, 9, 10), the density and the spin moment experience no perceptible changes at all. Slight changes in rows 2 and 3 of the table are due merely to variations in the orbital 'motion' of either state, because for both values of $\boldsymbol{k}$ the states remain noninteracting (see table 1). Interactions between the states of rows 6 and 8 persist, but the degree of mixing of spins with those of opposite signs decreases. Finally, interaction between states of rows 4 and 5 resulting from a symmetry change leads to their hybridization in spin and consequently to a decrease (in magnitude) of the spin moment of either state. It should be stressed that

the most significant changes in spin moment are not directly connected with variations of the energy term or the corresponding electron density, which are always small as seen from table 2.

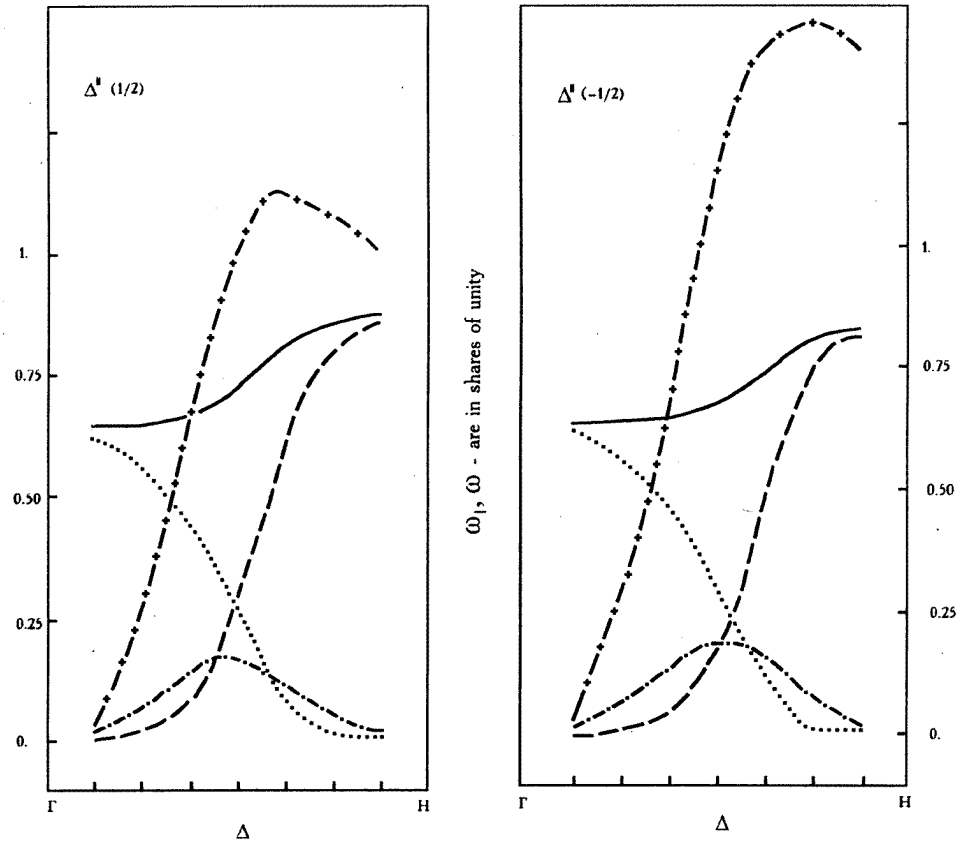


**Figure 2.** The electron density $\omega$ and its partial components $\omega_l$ inside the MT sphere versus $\boldsymbol{k}$ for the first and second energy bands. The solid curve represents $\omega$, where dotted, chain and dashed ones represent $\omega_0$, $\omega_1$, and $\omega_2$, respectively. The dispersion curves $E(\boldsymbol{k})$ (cross-and-dash) are plotted on an arbitrary (but the same) scale.

The electron density and its partial components inside the MT sphere are plotted in figure 2 for two lowest states $\Delta^{\|}(1/2)$ and $\Delta^{\|}(-1/2)$. Since the states do not interact, the corresponding electron densities evolve independently. Both states degenerate into s states at point Γ and d states at point H. At all intermediate $\boldsymbol{k}$-points all three types of component are present in the states. It can be seen from the plots that the s and d components vary monotonically in strict conformity with changes of the state type. Less natural seems the presence of a rather significant p component (up to 20% at the centre of the ΓH segment) for energies far removed from the p terms.

The electron spin moment and its partial components follow exactly (with an accuracy of 0.001) the trend of the density curve and the corresponding plots are just identical to those presented except for sign: the sign of the projection is positive for the states with $\tilde{\mu} = 1/2$ and negative for $\tilde{\mu} = -1/2$. Note, that the components of all three types are

equal spin carriers, so in this regard the d electrons do not stand out. We shall not discuss the states in the $\Delta^{\perp}$ direction, because in this case the results coincide with the preceding ones, even quantitatively.

## 5. The total spin moment for different quantum states

In [10] it was pointed out that weak spin–orbit interaction in Fe affects only slightly the magnitude of the energy terms and hence also the Fermi level position, energy band widths and density of states. It has already been shown (tables 1 and 2) that for the same reason the changes occurring in the energy and spatial density distribution are small for $\boldsymbol{k}$ parallel and normal to the magnetization direction. It was also mentioned that the spin magnetic moment in this state does not follow the density variation.

The calculations of the total spin moment for the $\boldsymbol{k}$-space directions parallel and normal to the magnetization ($\boldsymbol{k}_{\parallel}$ and $\boldsymbol{k}_{\perp}$) revealed a rather quaint picture of $\langle\sigma_z\rangle$ variation. The results of the calculations are shown in table 3. The bands are labelled in accordance with figure 1, while the $\boldsymbol{k}$-point numbering follows the division of the ΓH segment into subintervals $(1/8)(2\pi/a)$; the unnumbered rows correspond to intermediate $\boldsymbol{k}$-values.

First we consider the results in the top half of table 3. The states of the dispersion curve $1\parallel$ (see figure 1, left-hand page) have no nearby states of the same type and in the absence of interaction maintain $S_z$ close to 1. The dispersion curves $2\parallel$, $3\parallel$ and $4\parallel$ are essentially interacting, with the strongest hybridization of the states of bands $3\parallel$ and $4\parallel$ in the range are between the second and third $\boldsymbol{k}$-points. Since, however, for both states the values of $S_z$ are close to $-1$, hybridization does not lead to a change in $S_z$. At the same time, when the bands $2\parallel$ and $3\parallel$ approach each other in the range between the fourth and fifth $\boldsymbol{k}$-points, interaction of states with $S_z$ different in sign leads first to variation of the $S_z$-value and then to the change of its sign; for the band $2\parallel$ after intersection $S_z \approx -1$, and for the band $3\parallel$ $S_z \approx +1$. We should note that, firstly, all changes occur over a small $\boldsymbol{k}$-range and, secondly, there obviously exist $\boldsymbol{k}$-points where $S_z = 0$.

Because for $\boldsymbol{k} \perp \mathrm{O}z$ all states are already interacting, in the range between the fourth and fifth $\boldsymbol{k}$-points strong hybridization occurs for all three first bands. Now in this range for the third band, $3\perp$, $S_z$ changes its sign, as before, from '$-$' to '$+$'; however, the reversal of the sign of $S_z$ from '$+$' to '$-$' takes place not for the second but for the first band, $1\perp$. As to the second band $2\perp$, it plays the role of a 'mediator', having time to change the sign of $S_z$ twice. In other words, moving along $2\perp$, we twice run across the states with $S_z = 0$.

As seen from the bottom half of table 3, a similar situation arises for bands 3, 4 and 5 in figure 1, right-hand page. Without going into details, we only mention that again all the changes occur in the middle portion of the ΓH segment and—which is more interesting—near the Fermi surface.

## 6. Conclusion

The implication of the analysis performed may be stated as follows. The consideration of the state symmetry allows us to determine more correctly the compatibility of energy bands and, in particular, to analyse the distributions between the dispersion curves for the BZ directions parallel and normal to the magnetization. It is shown that for isolated energy bands the spin density in FM-Fe follows the charge density deviations; this is also true for an arbitrarily strong interaction between states with the same preferred spin direction. At the same time, for even weak interaction of states with opposite spin directions the spin density

**Table 3.** The projection of the spin magnetic moment onto the $Oz$ axis (in $\mu_B$).

| | Energy bands[a] | | | | | |
|---|---|---|---|---|---|---|
| $\boldsymbol{k}$[b] | 1‖ | 1⊥ | 2‖ | 2⊥ | 3‖ | 3⊥ |
| Γ | 0.999 | 0.999 | 0.998 | 0.998 | −0.999 | −0.999 |
| 1 | 0.999 | 0.999 | 0.998 | 0.998 | −0.999 | −0.999 |
| 2 | 0.999 | 0.999 | 0.998 | 0.998 | −0.999 | −0.998 |
| | 0.999 | 0.998 | 0.998 | 0.997 | −0.998 | −0.998 |
| 3 | 0.999 | 0.998 | 0.998 | 0.995 | −0.998 | −0.997 |
| | 0.999 | 0.998 | 0.998 | 0.989 | −0.998 | −0.989 |
| 4 | 0.999 | 0.997 | 0.995 | 0.909 | −0.996 | −0.908 |
| | 0.999 | 0.983 | 0.964 | −0.936 | −0.965 | 0.950 |
| 5 | 0.998 | −0.974 | −0.973 | 0.979 | 0.972 | 0.991 |
| | 0.998 | −0.995 | −0.996 | 0.996 | 0.996 | 0.996 |
| 6 | 0.998 | −0.998 | −0.998 | 0.998 | 0.998 | 0.997 |
| 7 | 0.998 | −0.999 | −0.999 | 0.998 | 0.998 | 0.998 |
| H | 0.999 | −0.999 | −0.999 | 0.999 | 0.998 | 0.998 |
| | Energy bands[c] | | | | | |
| $\boldsymbol{k}$[b] | 3‖ | 3⊥ | 4‖ | 4⊥ | 5‖ | 5⊥ |
| Γ | 0.967 | 0.991 | −0.967 | −0.967 | −0.990 | −0.990 |
| 1 | 0.960 | 0.982 | −0.960 | −0.974 | −0.993 | −0.991 |
| 2 | 0.932 | 0.970 | −0.932 | −0.967 | −0.996 | −0.996 |
| | 0.902 | 0.956 | −0.902 | −0.954 | −0.997 | −0.997 |
| 3 | 0.829 | 0.923 | −0.829 | −0.922 | −0.997 | −0.998 |
| | 0.450 | 0.707 | −0.450 | −0.706 | −0.997 | −0.998 |
| 4 | −0.814 | −0.864 | 0.814 | 0.866 | −0.997 | −0.998 |
| | −0.981 | −0.988 | 0.981 | 0.990 | −0.997 | −1.0 |
| 5 | −0.995 | −0.997 | 0.995 | −0.999 | −0.997 | 0.997 |
| | −0.998 | −0.998 | 0.998 | −0.999 | −0.997 | 0.999 |
| 6 | −1.0 | −1.0 | 0.999 | −0.999 | −0.999 | 0.999 |
| 7 | −1.0 | −1.0 | 0.997 | −0.999 | −0.999 | 0.998 |
| H | −1.0 | −1.0 | —- | −0.999 | −0.999 | — |

[a] The numbering of bands corresponds to figure 1, left-hand page.
[b] The numbering of the $\boldsymbol{k}$-points corresponds to the division of the ΓH segment into eight parts.
[c] The numbering of the bands corresponds to figure 1, right-hand page.

does not follow the charge density—changing the sign of the spin from point to point in the BZ and vanishing at individual $\boldsymbol{k}$-points. When there is interaction of several states with differing spin direction, the general picture of $S_z(\boldsymbol{k})$ variation can be quite complicated.

The above-mentioned facts are of little importance as long as characteristics connected with integration over the filled portion of the spectrum are calculated. However, in analysing phenomena due to the motion of an electron over the Fermi surface the band compatibility and individual state characteristics can play a crucial role.

## Acknowledgment

The authors are very grateful to their colleagues S A Ostanin and V Yu Trubitsin for the supply of some computer programs and help with the calculations.

## References

[1] Feder R, Rosicky F and Ackermann B 1983 *Z. Phys.* B **52** 31
[2] Strange P, Staunton J B and Gyorffy B L 1984 *J. Phys. C: Solid State Phys.* **17** 3355
[3] Ostanin S A and Shirokovskii V P 1990 *J. Phys.: Condens. Matter* **2** 7585
[4] Takada S 1966 *Prog. Theor. Phys.* **36** 224
[5] Onodera J and Okazaki M 1966 *J. Phys. Soc. Japan* **21** 1273
[6] Strange P, Ebert H, Staunton J B and Gyorffy B L 1989 *J. Phys.: Condens. Matter* **1** 2959
[7] Ackermann B, Feder R and Tamura E 1984 *J. Phys. F: Met. Phys.* **14** L173
[8] Strange P, Staunton J B, Gyorffy B L and Ebert H 1991 *Physica* B **172** 51
[9] Guo G Y, Temmerman W M and Ebert H 1991 *Physica* B **172** 61
[10] Ostanin S A and Shirokovskii V P 1992 *J. Phys.: Condens. Matter* **4** 497
[11] Shirokovskii V P and Shilkova N A 1982 *Fiz. Metall. Metalloved.* **54** 218
Ostanin S A, Trubitsin V Yu, Shilkova N A and Shirokovskii V P 1987 *Fiz. Metall. Metalloved.* **64** 421
[12] Shirokovskii V P, Shilkova N A and Trubitsina N A 1986 *Phys. Status Solidi* b **133** 593
Shilkova N A and Shirokovskii V P 1988 *Phys. Status Solidi* b **149** 571
[13] Shilkova N A, Shirokovskii V P and Trubitsin V Yu 1992 *Phys. Status Solidi* b **172** 627
[14] Ham F S and Segall B 1961 *Phys. Rev.* **124** 1786
[15] Bouckaert L P, Smoluchowskii R and Wigner E 1936 *Phys. Rev.* **50** 58
[16] Hörmandinger G and Weinberger P 1992 *J. Phys.: Condens. Matter* **4** 2185